Coarsening of axial segregation patterns of slurries in a horizontally rotating drum

Tilo Finger,[1] Andreas Voigt,[2] Jörg Stadler,[3] Heiko G. Niessen,[4] Lama Naji,[1] and Ralf Stannarius[1]
[1]*Otto-von-Guericke-University, Institute of Experimental Physics, Universitätsplatz 2, D-39106 Magdeburg, Germany*
[2]*Max-Planck-Institute for Dynamics of Complex Technical Systems, Sandtorstraße 1, D-39106 Magdeburg, Germany*
[3]*Leibniz Institute for Neurobiology, Brenneckestraße 6, D-39118 Magdeburg, Germany*
[4]*Center of Advanced Imaging (CAI) and Department of Neurology II, Otto-von-Guericke-University, Leipziger Straße 44, D-39120 Magdeburg, Germany*
(Received 27 September 2005; revised manuscript received 30 January 2006; published 29 September 2006)

Segregation structures of granular mixtures in rotating drums represent classical examples of pattern formation in granular material. We investigate the coarsening of axial segregation patterns of slurries in a long horizontally rotating cylinder. The dynamics and the three-dimensional geometry of the segregation structures are analyzed with optical methods and nuclear magnetic resonance imaging. Previous studies have mainly considered global statistical features of the pattern dynamics. In order to get insight into driving mechanisms for the coarsening process, we focus on the details of the dissolution of individual bands. We treat the coarsening as a consequence of interactions of adjacent bands in the pattern, which are determined by their geometrical relations. In addition to initially homogeneous mixtures, which evolve to spontaneously formed patterns, we study the evolution of specially prepared simple initial states. The role of the three-dimensional geometry of the axial core in the dissolution process of segregation bands is demonstrated. Relations between geometry and dynamic processes are established, which may help to find the correct microscopic models for the coarsening mechanism.

DOI: 10.1103/PhysRevE.74.031312 PACS number(s): 45.70.Mg, 45.70.Qj, 05.65.+b, 83.85.Fg

I. INTRODUCTION

Segregation processes in mixtures of granular materials represent a fascinating research topic, with many unresolved fundamental questions. Segregation phenomena in such materials are ubiquitous in everyday life, in technological processes, as well as in very simple model systems [1–3]. In particular, the dynamics of granular mixtures in horizontally rotating drums have attracted the interest of experimental and theoretical researchers. The system is particularly simple in its geometrical construction and its preparation, and the observation techniques are straightforward.

Axial segregation has first been described more than 60 years ago [4] and it has been studied extensively during the last decade. Experiments have been performed under various geometrical conditions and with a wide variety of material compositions [4–26]. These experiments have provided an abundance of experimental data. Different theoretical descriptions have been developed, including numerical simulations and analytical models [26–39]. Nevertheless, the system dynamics are far from being fully understood. One of the reasons for that may be the large variety of influences that may have to be considered, but apart from that there is certainly a lack of fundamental understanding of granular dynamics in general. Many features of the segregation and coarsening processes are still not satisfactorily described.

In the systems considered here ("slowly" rotating drums, see below), the redistribution of grains in the granular bed is largely restricted to a shallow surface layer [40]. The majority of investigations have focused on the segregation of bimodal mixtures of spherical beads, but systems with ellipsoidally or irregularly shaped grains, e.g., Refs. [19,20], and polydisperse mixtures have been studied as well. Details of the dynamics of the segregation pattern depend crucially upon the conditions of the experiment. Traveling-wave-like patterns [19,20], "wavy" patterns [23], and stationary stripes (e.g., Refs. [22,23]) have been described, for example. The reversibility of the axial segregation processes has been demonstrated [13,14]. The qualitative and quantitative characteristics of the segregation and coarsening dynamics is sensitively influenced by many parameters. Geometry and size distribution of the particles, densities, and masses, rotation speed of the drum (i.e., energy supply per time), and the filling factor play a role, as well as the environment (dry or wet surroundings). Most of the experiments have been performed in dry systems where the grains are immersed in air; only a few experiments deal with granulates [41,42] or granular mixtures [21–23] immersed in a liquid of lower density (slurries).

The segregation phenomena observed in a horizontally rotating long mixer, filled initially with a homogeneous mixture of different-sized granulate, can be roughly separated in three periods. Initially, during one or a few rotations, one observes a radial segregation of the material [43], where small-sized particles collect in an axial core of the granulate, while the large-sized component accumulates in the outer region. In a subsequent period of the order of a hundred rotations, axial segregation sets in. The core becomes modulated until the fine-grained material develops a band pattern [12,15,16]. Axial segments are formed where the large-sized particles are more or less completely replaced by the small-sized components of the mixture. Such bands alternate with regions where only a narrow core of small particles is embedded in a surrounding shell of large particles. As the driving factor for this axial structuring process, differences in the dynamic angles of repose of mixed and segregated granulate have been suggested [13]. The following period is character-

ized by the coarsening of the band pattern. Individual bands merge and the number of bands decreases continuously. The dynamics of this coarsening process are much slower than those of the preceding processes. It is reasonable to assume that coarsening continues until the material is completely sorted into one compartment containing small-sized particles and a second compartment of large particles enclosing a core mainly formed by small-sized particles. However, the time scales on which the system approaches a final stationary state are much longer than the typical runs of the experiments in this study, hence we have not tested whether this hypothesis is globally justified.

We focus here on bimodal mixtures of spherical glass beads entirely submerged in a liquid in a long cylindrical drum. The two species of beads have identical densities, but different radii. The experiments are performed at Froude numbers $\mathrm{Fr} \ll 1$. The Froude number ($\mathrm{Fr}=R\omega^2/g$, where ω is the angular velocity of the drum, g is the gravitational acceleration, and R is the tube radius) is a measure for the ratio of inertial and gravitational forces. The process of the formation of axially segregated bands in this dynamic range has been studied intensively, in particular in dry systems, whereas the long-term stability of the segregation patterns is not well understood. The coarsening process has been described, e.g., in dry systems [11,15,16,22], but also in slurries [22,23]. A logarithmic decay law for the number of bands in the drum has been discovered by Fiedor *et al.* [22]. It is equally suited to describe the coarsening dynamics in dry and wet systems, even though the parameters differ considerably between the two types. Influences of the filling factor of the mixer have been investigated in slurries by Arndt *et al.* [23]. Evidently, the filling level has important consequences there for the formation and persistence of the core of small particles when the axial segregation structures appear.

To date, a comparison of dry systems with granular mixtures enclosed in a liquid environment (slurries) on the basis of available experimental data gives no clear picture of the influences of the immersion liquid. Slurries, as studied here, are interesting for themselves because of their relevance in a number of technical applications. Axial segregation appears to be significantly faster in slurries [22] in comparison to the dry counterpart. Fiedor *et al.* [22] have pointed out that there are qualitative differences between dry and wet systems. Interesting aspects are discovered when the parameter space of rotation rates is analyzed: In dry systems it has been reported that at the slowest possible speed (above the avalanche regime), the system does not segregate axially during the observation period. At higher rotation rates, a regime with extremely fast segregation is found, and no coarsening occurs during the entire experiment. Then, with further increasing rates, the system enters the so-called standard coarsening regime, whereas at the highest velocities studied, complex dynamical patterns, including traveling waves, appear. In comparison, slurries studied in Ref. [22] produce the segregation patterns generally at lower rotation rates. The experiments indicate that axial segregation in slurries is quite robust. The wet systems seem to suppress traveling waves and favor the spatial fixation of segregation patterns. The fraction of small-sized particles visible on the surface of the glanular mixture is systematically higher in the wet systems [22]. The changes in the relative widths of visible bands suggest significant changes in the interior composition of the segregation structures.

Simulations with molecular-dynamics methods have led to predictions of the three-dimensional structure of the segregation patterns in dry systems [33,37]. The authors of these studies present calculated snapshots of the three-dimensional (3D) segregation structure during the coarsening process. Experiments with optical methods [23] and nuclear magnetic resonance (NMR) [10,15,16] have been employed to elucidate such subsurface structures in different systems. To date, however, there has been no commonly accepted explanation of the relation between individual band geometry, stability, and coarsening dynamics.

In this study, we investigate experimentally the long-term dynamics of axially segregated bands in slurries, in particular, their stability, their internal structure, and the process of their dissolution. In the first part, we record the dynamics of stripe patterns that form spontaneously from a completely mixed initial state. In the subsequent part, we prepare regular band patterns as initial states in the mixer and analyze their dynamics in order to understand details of the coarsening process.

The segregation patterns are investigated optically and by means of magnetic resonance imaging (MRI). The presence of water as the embedding fluid is not interesting only because of the similarity of this system to a number of technical applications. It also facilitates, in combination with the magnetic-resonance-insensitive granulate, the MRI investigation of the 3D segregation structures by the water distribution in the tube.

We discuss the following details of the coarsening process: How do the long-term dynamics depend upon the rotation velocity? How does an individual band in a segregated pattern evolve and finally disappear? What determines the stability of bands? Is there a relation between the 3D band geometry and its dissolution? In particular, we try to establish relations between sizes and geometries of individual stripes and their evolution in the dynamic coarsening process.

The experimental conditions are described in the next section. In Sec. III, we give a brief review of the experimental observations during the evolution of the axial stripes and their dependence upon experimental parameters, and we discuss the long-term coarsening dynamics of the patterns. In Sec. IV, the preparation and study of regular band structures is described, and the dissolution of bands is analyzed optically. Section V describes a 3D analysis of the band structure by means of nuclear magnetic resonance imaging, and Sec. VI summarizes the experimental results and derives the conclusions.

II. EXPERIMENT

As stated above, granular mixtures in the horizontal rotating drum can be studied under very different conditions. In our experiment, the granulate is completely immersed in water. The rotation speed is slow (well below 1 rpm), so that the motion of the granulate is essentially restricted to sliding

in a fluidized top layer. The mixtures consist of spherical glass beads with bimodal radius distribution, where the radii of large and small particles were approximately 3:1 in mixture L, with large spheres of 1.5 mm and small spheres of $\approx$0.55 mm diameter. If not otherwise indicated, experiments are performed with this mixture. In mixture S, which is composed of large spheres of 1.5 mm and small spheres of $\approx$0.75 mm diameter, this ratio is 2:1. While the large-sized particles in both mixtures are practically monodisperse, the small-sized components have been obtained from sieving fractions. Their diameters are distributed between 0.50 and 0.63 mm for the first mixture, and between 0.71 mm and 0.80 mm for the second mixture. The initially homogeneous mixtures were prepared with 50%:50% (tapped volume) mixtures of both species, respectively.

The mixer consists of a cylindrical Duran glass tube (*Schott*) with an inner diameter of $d=36.8$ mm. Drums of three different lengths have been used. Measurements with prepared single stripes or stripe pairs were performed in a 662 mm ($18d$) drum. The experiments reported for initially homogeneous mixtures were performed in a 994 mm ($27d$) drum. Additional experiments with initially homogeneous mixtures in the 662 and 332 mm drums have been performed in order to test influences of the finite drum length. These experiments confirmed that for the standard coarsening dynamics in the central region of the drums, excluding regions of about $1\cdots2d$ at the tube ends, boundary effects can be neglected (cf., however, the fast speed regime with stable bands in the tube center, Fig. 3, which is described below). In all experiments, the fill level of granulate was 1/2, i.e., the dry mixture occupies one half of the drum volume. After loading the granulate, water is subsequently filled up into the tube. It is closed tightly at both ends, with an aluminum plug on the motor side (right-hand side in the images), and a teflon plug on the opposite side. A benefit of the presence of water is that there is no electrostatic charging of the granulate during the experiment. It is essential for the formation of the segregation bands and the character of the coarsening process that the initial mixture is as homogeneous as possible.

Great care has been devoted, in particular, to the development of a technique that avoids demixing during the tube filling. In the experiments with well-mixed granulate, a good criterion for the quality of the filling process is the regularity of the band texture that forms after the first few dozen rotations. If the granulate has not been well mixed initially, then the texture of stripes is not regular on a large scale; the density of bands will then vary along the drum axis. An example of a quite regular initial band structure may be seen in Fig. 2.

The technique used for the preparation of the regular stripe patterns is as follows: one end of the drum is closed by a plug. Then, an aluminum plate of the length of the tube and the width of the inner tube diameter is inserted into the tube. It bisects the inner tube volume in exactly two halves, one of the half-cylindrical free volumes is filled with the granulate by stuffing the mixture into the tube. After this free volume is completely filled, the plate is removed, the tube is slowly filled up with water, and its end is closed.

The setup for optical investigations is depicted in Fig. 1. The mixer is held in an exact horizontal position by pairs of

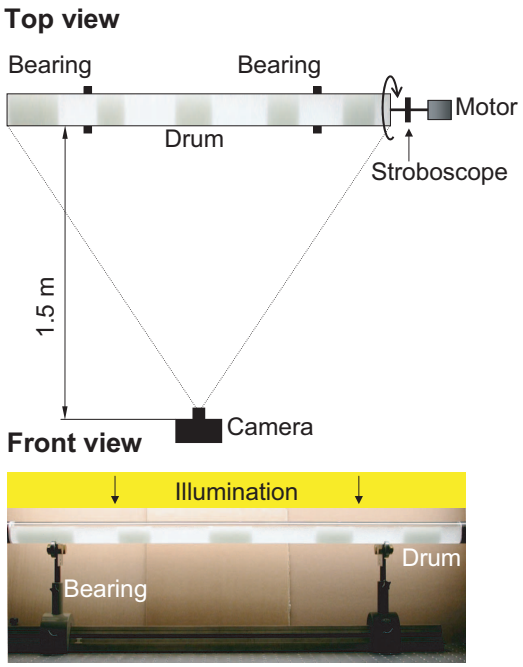

FIG. 1. (Color online) Sketch of the experimental setup. The drum rests on two ball bearings on each side; it is driven by a dc motor. The rotation speed is monitored by a stroboscopic counter. The drum is illuminated from the top. A digital camera at the same height as the drum, positioned in a distance of 150 cm, automatically takes photos at regular intervals. The width of the drum shown is $\approx$1 m. For a typical experiment, the observation time ranges between one day and one week.

supporting ball bearings; two bearings on each side fix the drum axis. The drum is rotated by a dc motor with a speed-reduction gear at rotation speeds between 5 and 30 rpm. The rotation speed is continuously monitored with a stroboscopic disk on the mixer axis and a photodiode.

The drum is uniformly illuminated from the top and images are taken in regular time intervals by means of a Nikon Coolpix 990 digital camera controlled by a computer program. The direction of rotation is such that the camera sees the "back" of the pattern, i.e., the slope of the granulate is directed away from the camera. Typically, the time intervals between the images are 30 s in the initial phase of the experiment, while at later stages the time intervals are increased because of the logarithmic dynamics of the coarsening processes. Digital images are processed by standard software (MATLAB). Depending upon the rotation speed and the initial conditions, the time frame of a single experimental run is one day to about one week. In most experiments, a final stationary state of the segregation pattern is not yet reached after that time.

For the study of the 3D geometry of the segregation structures by means of MRI, the rotation of the tube has been stopped at regular intervals and sagittal as well as axial cross sections [44] of the water distribution in the tube have been measured by means of a Bruker BioSpec 47/20 MRI scanner operating at 200 MHz proton resonance frequency (4.7 T). MR images were measured with a T_2 (transverse relaxation time) weighted sequence. Water appears bright and the beads

FIG. 2. Axial segregation pattern of a 50%:50% mixture of glass beads, after 20 min at 15 rpm. Dark areas represent bands of small particles; bright bands contain large particles at the surface. The width of the drum is ≈1 m.

appear dark in the images. The tube was inserted horizontally into the receiver coil with an opening of about 7 cm; the length of the sensitive volume was about 8 cm. Although the complete tube cannot be monitored with a single MRI experiment, local details of the band structure can be monitored. For the measurement of longer sections of the drum, the sample has to be shifted in the MRI spectrometer and images have to be composed from multiple measurements at different positions of the tube. The spatial resolution of the MRI experiment was approximately 0.5 mm. Thus, individual glass beads of the large species can be clearly resolved, while the small beads are at the limits of resolution. In earlier MRI experiments, Hill *et al.*, for example, have used MRI-sensitive granulates (containing protons) which are mapped positively in the MR images, whereas in our experiment, the granulate does not give a magnetic resonance signal. The granular particles appear negative in the MR images, while the proton signal originates from the water phase.

III. SEGREGATION AND COARSENING OF INITIALLY HOMOGENEOUS MIXTURES

Figure 2 shows a typical image of the drum after 300 rotations at a speed of 15 rpm (revolutions per minute). The reflection of the granulate is essentially determined by the local composition of the mixture. Regions containing small beads appear darker in the transmission images. The outer regions of the granulate in the direction towards the camera have a much greater influence on the brightness than the central and rear parts, so the optical images reflect, to a large degree, the composition of the granulate near the glass surface. The dark regions reflect parts of the tube filled with small spheres, and regions where the tube is filled with the large particles, at least in the outer parts, appear bright. The existence of a small axial core of different structure does not influence the optical appearance in our experiments, thus it has to be detected with alternative methods (MRI experiments). We disregard the first stages of the segregation, which have been described in detail by other authors, and concentrate here on the fully developed band patterns. The evolution of these bands is shown in Figs. 3(a)–3(c) where the formation of the core and the axial segregation occur during the very first rotations (hardly resolved in the plots). The spatiotemporal plots are obtained, as usual, by selecting horizontal cross sections of the drum in a sequence of images recorded in regular time intervals (several horizontal pixel rows in the digitized images are averaged). These optical profiles are composed into a two-dimensional plot. The vertical axis, running from top to bottom, is the time axis, and

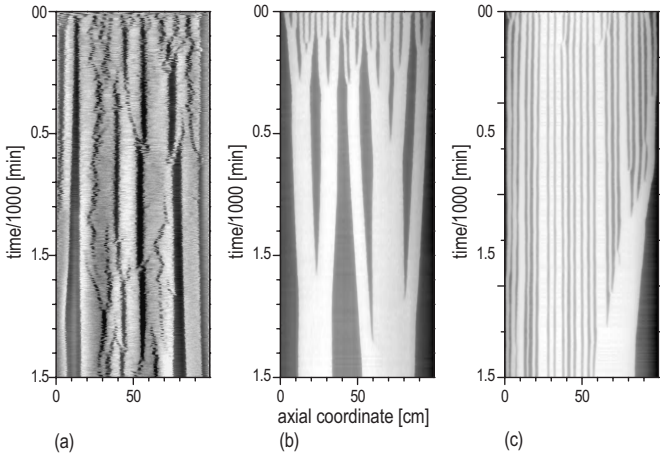

FIG. 3. Spatiotemporal presentation of the stripe evolution for mixture *L* and the 994 mm drum for three different rotation speeds; (a) 5 rpm, (b) 15 rpm, (c) 30 rpm. Time runs from top to bottom.

the horizontal axis comprises the full length of the tube. The images correspond to the three characteristic regimes that are found, depending upon the rotation speed. Figure 3(a) is typical for a slow rotation speed of the tube. In this case, no stable band pattern is formed, but the smaller beads collect in irregular, nonstationary clouds. Such clusters can form spontaneously and disappear again; their position is not fixed. Another typical feature of the slow-rotation experiments is that larger clusters of the small beads have a higher stability than small aggregates, as is evident in the figure.

Above a certain rotation speed of about 10 rpm, regular stripes appear. The number of stripes (of small particles) is slightly larger than the aspect ratio of drum length to diameter. The initial pattern of more or less equidistant stripes decays with a logarithmic dependence upon the number of rotations. Figure 3(b) evidences that the characteristic feature of this regime is the apparently random dissolution of individual stripes. The small beads contained in the dissolving stripes are distributed between the neighboring bands of small beads in the array. The decay rate (number of stripes per rotation) determined statistically is practically independent of the rotation speed in a certain parameter range. Figure 4(a) shows a representative collection of experimental data; the number of stripes N is given as a function of the number of rotations r for different rotation speeds in a semilogarithmic plot. The initial number of stripes is relatively insensitive to the speed of rotation, but a certain tendency is indicated that more stripes are formed at higher rotation speeds. The formation of the stripes occurs faster (smaller number of rotations) at higher rotation speeds. The fit of $N(r)$ is not very sensitive to the rotation speed in the parameter range between approximately 10 and 22 rpm; it can be fitted for the 1 m drum with the logarithmic dependence

$$N(r) = N_0(1 - n \ln r) \text{ with } N_0 = 55, \quad n = 0.092.$$

In the semilogarithmic coarsening plot of Fig. 4(a), this fit is shown by a linear graph, which describes the experimental data reasonably well after an initial period of ≈100 rotations. In the range of rotation speeds shown in the plot, the devel-

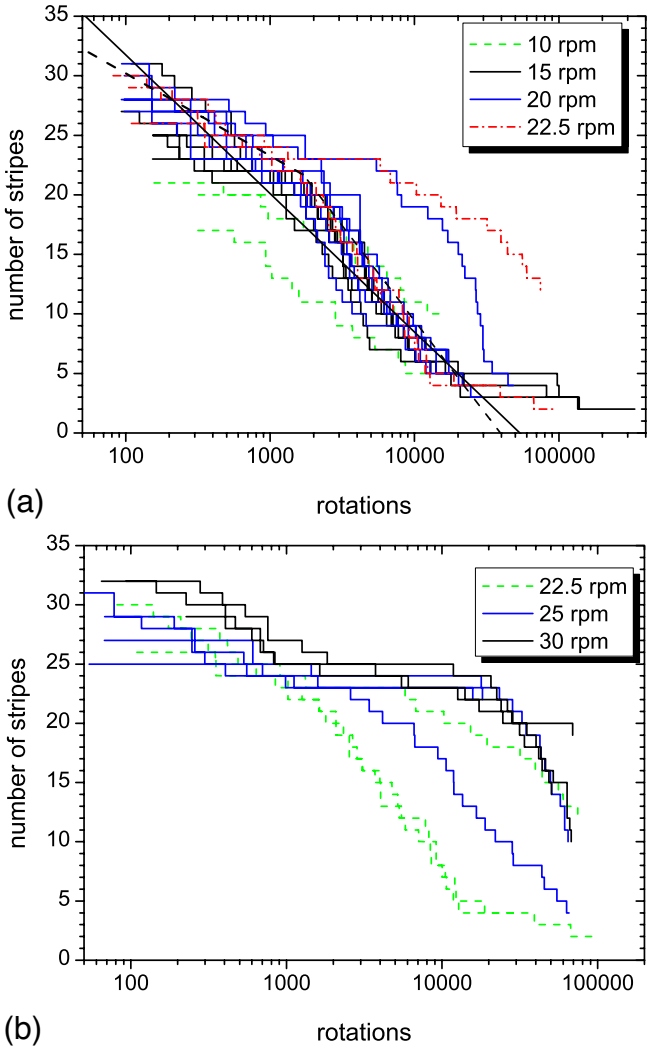

FIG. 4. (Color online) Number of stripes N in a 994 mm long half-filled tube (mixture L) as a function of time for different rotation speeds of the drum. Plot (a) contains data for intermediate rotation rates (10 to 22.5 rpm). The data follow a logarithmic decay, with few exceptions for high rotation rates. The plot (b) collects the data for high rotation rates; with increasing rotation rate the tendency to form a plateau (stationary pattern) is exhibited. There are data from 21 individual experimental runs in plot (a), and in addition 10 runs in plot (b).

opment of the number of stripes in a segregation pattern can be described with this universal dependence. There are only a few deviations at high rotation rates, at the transition to the next regime. The initial stripe number is approximately 30 per meter tube, i.e., the initial period of the pattern is $\approx 0.9\times$ the drum diameter. The initial number of stripes varies in individual experiments with the same rotation rate by about 10%. In addition, there is the systematic decay of the number of stripes with decreasing rotation rate (see Fig. 4).

For comparison with the experimental results given in Ref. [22], one has to consider that we define the constant n in a different way, accounting for the fact that N_0, and consequently the decay of $N(r)$, is proportional to the tube length. N_0 is not given in Ref. [22], but if one takes experimental data from Fig. 3 in Ref. [22], one arrives at $n \approx 0.095$ for the circular slurry drum, in agreement with our results.

A closer inspection of the experimental data reveals that the simple logarithmic dependence is only a first approximation. In the late stage of the experiment, when only a couple of bands (2 or 3 bands of small beads) are left, influences of the lateral edges of the mixer gain significance. The experimental data deviate systematically from this fit curve towards larger N, i.e., the final coarsening is significantly slower than expected from the fit.

A refined analysis also shows that the graphs of Fig. 4(a) actually indicate a certain bend after about 2000 rotations, when the number of bands in the texture has decreased to approximately 2/3 of the initial value. The negative slope of the logarithmic decay increases. The initial value for n is approximately 0.06, while in the second part it reaches $n \approx 0.125$. Dashed lines in Fig. 4(a) visualize these initial and later slopes. This acceleration of the coarsening process is characteristic for all individual curves. Fiedor and Ottino [22] who have investigated a similar system have not reported this detail. In their study, however, the experiments have been performed over a much shorter time period; their record ends where the initial number of stripes has decreased to about 1/2.

Figure 3(c) shows the behavior at rotation speeds above 22 rpm. The stripes in the texture vanish on a much slower time scale, and with a qualitatively different scenario. The dissolution of individual stripes is not random, but stripes disappear sequentially from one side. This suggests that the process leading to dissolution is different; there is no real coarsening of the pattern. The individual bands in a perfect array seem to be stable at high-rotation speeds. However, at a finite tube length the influences of the tube ends become essential. The stripes are destroyed one by one starting from one or both tube ends. From that observation it seems that (although we are not able to test this prediction experimentally) the initially segregated short-wavelength band structure in a very long tube would be stable. Only the broken translational symmetry at the tube ends lead to the gradual destruction of the band pattern, and the fine-grained material collects at the tube ends. In the spatiotemporal plot of Fig. 4(b) it is seen that the band structure persists much longer than in the experiments with a slower rotation rate; the $N(t)$ graphs contain very extended horizontal segments (note the logarithmic time scale).

Another feature of the spatiotemporal behavior is evident in Figs. 3(b) and 3(c). Only the bands with small beads change their width, while the bands containing large beads (bright stripes) retain a constant size, or merge to form bands with widths equal to the sum of the merging regions. This indicates that the stripe-pattern evolution is mediated only by redistribution of the small beads through the channel structure of the axial core, while on the other hand, the bands of small beads represent barriers for the diffusion of large beads. In detail, it is once more emphasized in Fig. 5. One may show by a simple geometrical argument that the bands of small-sized grains form barriers for the large grains in our mixture: If one takes any axial drum position that is occupied by small beads during the complete run of the experiment (for example, at the axial positions 38 or 75 cm in Fig. 5), then the relative amounts of large beads on both sides of

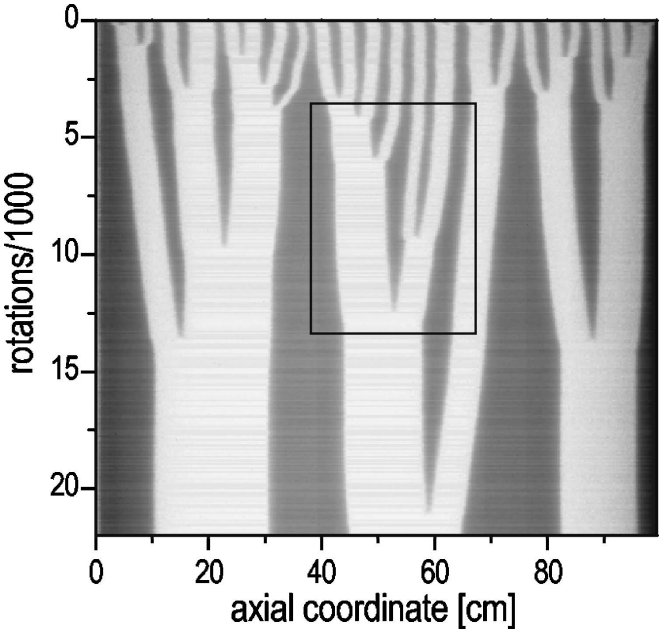

FIG. 5. Spatiotemporal plot of the evolution of segregation patterns in a bidisperse mixture of small and large glass beads (mixture *L* at 20 rpm). Note that in an array of stripes, usually the narrow dark stripes dissolve first, their material is distributed among the neighboring stripes. The box highlights a selection that is discussed in detail in the text. Some slight intensity fluctuations in the time domain are artifacts due to contrast variations between individual photos, which have not been corrected in this plot.

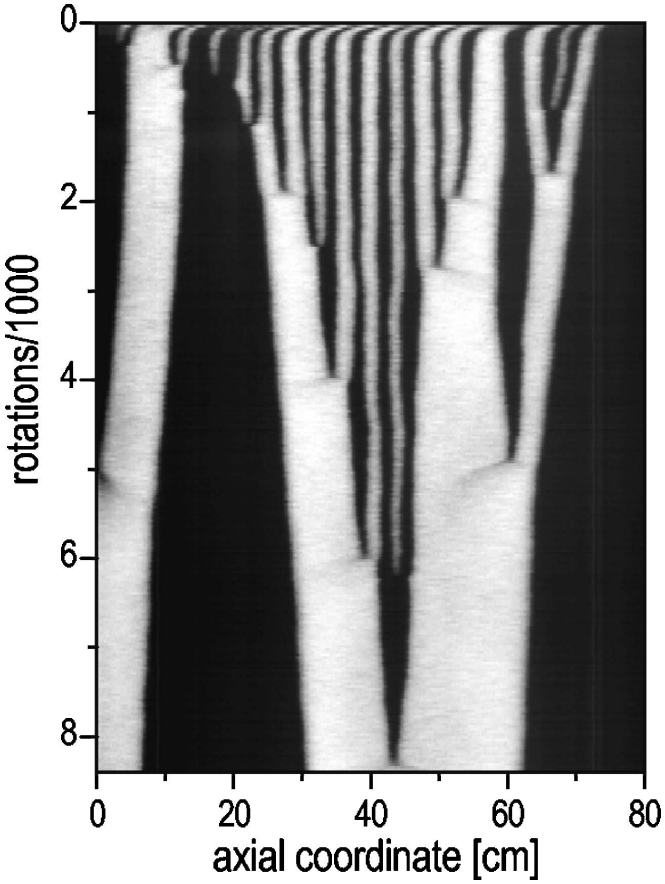

FIG. 6. Spatiotemporal plot of the evolution of segregation patterns in a mixture of sand and large (diameter 2 mm) glass beads, 15 rpm. Both the dark and bright bands can dissolve in the coarsening process. The large particles contained in the bright stripes can penetrate the dark zones of polydisperse irregular small-grained particles.

each of these positions are constant at all times in the spatiotemporal plot. The geometrical argument is only statistical evidence, and the exchange of large particles through bands of narrow particles could be present if it occurred at equal rates in both directions. However, the MRI measurements in Sec. V will confirm our barrier assumption. It will be shown that the regions that contain small beads are completely free of large beads. We note that this seems to be a peculiarity of certain bidisperse mixtures. It cannot be generalized. For comparison, Fig. 6 shows an experimental space-time plot of a mixture containing glass beads (bright regions) of 2 mm diameter and fine-grained sand (polydisperse irregular particles, diameter less than 0.5 mm) as the second component, in a 50%:50% (tapped volume) mixture. It is obvious that in this experiment, the topology of the texture evolution is qualitatively different from the bidisperse mixture. Both the dark stripes (sand) and the bright stripes (glass beads) can dissolve after the initial axial segregation process, and the width of the bands of large beads fluctuates considerably with time. In this case, where the small particles are not regular monodisperse spheres, the large particles migrate through the regions of small particles. The treatment of this case, involving two diffusion processes, seems much more complex than the case of our bimodal sphere mixtures, and we will not consider it further in this study. Taking a look at space-time plots published in literature, one can find evidence that this barrier effect is found in other granular mixtures, too [22,23], but there are also counterexamples showing that in some systems large grains may penetrate the regions formed by small grains [9,15]. Additional experiments are necessary to investigate this detail. It is not clear, at the moment, whether the main reason for this qualitatively different coarsening scenario is the size distribution of the small component or the small size. Nevertheless, the image serves as a demonstration that the blocking of large-particle redistribution by the small-particle bands is not universal for all types of granulates.

Figure 5 draws attention to the dissolution of individual bands in the stripe pattern of the bidisperse mixtures. It is apparent that in most of the cases, narrower stripes start to dissolve when their neighbors have a considerably larger width (see framed section), so the broader stripes grow at the expense of narrower ones. The central stripe in the boxed area grows, as long as it is flanked by narrow neighbors; it collects their content of small-sized particles. Only after these narrow stripes have disappeared, the neighboring stripes are much broader and the stripe loses material until it is extinct. However, this rule of the material transport from narrow to broad stripes is not strict, in some parts of the spatiotemporal plot one can see that narrower stripes grow at the expense of their initially somewhat broader neighbors. An even more striking observation is that if one stripe starts

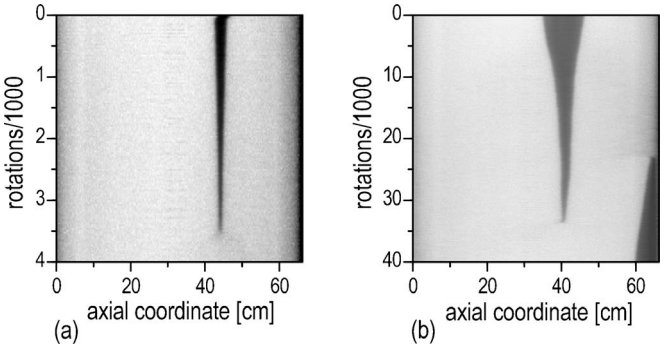

FIG. 7. Spatiotemporal plot of the evolution of single prepared stripes of fine beads surrounded by large beads. (a) Small stripe; the material dissolves and forms a core structure. (b) The core extends to the lateral end of the drum where the small beads are collected in a stripe again. The tube length is 662 mm. The stripes have initial widths of 4 cm (a) and 12 cm (b), respectively, and their right edge is initially 20 cm from the tube end.

to grow at the expense of its neighbors, the process is irreversible. The transport of the small-sized particles, once established, continues until the shrinking stripe is extinct.

In a spontaneously formed band texture these effects are hard to separate, since each band interacts with both neighbors, and those are in interaction with their neighbors in turn. Consequently, we have changed the initial conditions of the experiment and prepared well-defined initial band structures of few stripes. The custom-made filling device described above allows us to prepare tubes with clearly defined initial conditions.

IV. EVOLUTION OF PREPARED REGULAR PATTERNS

Small- and large-sized beads are alternatvely filled into the horizontal drum so that the initial state is a sequence of bands of small-sized beads, separated by bands of the large-sized beads. The advantage of this procedure is that we can observe the separate interaction of two bands once the axial core has formed. It goes without saying that in these experiments, the ratio of the amount of small-sized to large-sized beads is not 1:1. If not explicitly stated otherwise, the experiments with prepared initial patterns are performed at 15 rpm.

A first set of experiments, with single stripes of small beads, is shown in Figs. 7(a) and 7(b). With the term stripe, we refer in the following, in short, to the bands of small-sized material. A single narrow stripe of small beads dissolves and the material is spread in an axial core along the drum [Fig. 7(a)]. The small amount of material submerges completely. In the experiment shown in Fig. 7(b), the fine-grained material has formed a core that extends to one side of the tube, where a substantial share of the material reappears in a band at the tube end, while the original band disappears. The experiment gives a rough estimate of the time scales of the following dynamic processes. The initial rate of the stripe dissolution is the same for both the narrow and the broad stripe. The material lost by the stripes submerges in the invisible core structure. One may conclude that the velocity of the core formation is independent of the width

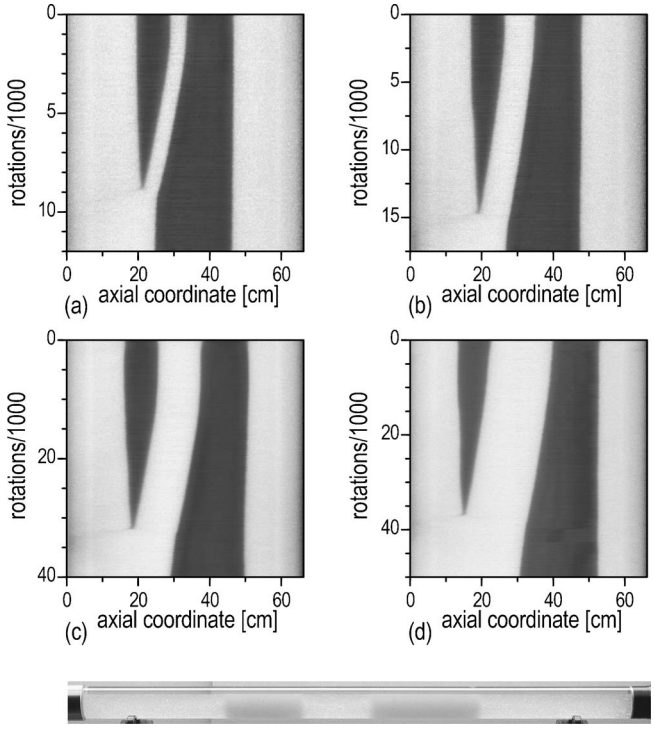

FIG. 8. The image on the top shows a tube with two prepared stripes of small-sized beads of 105 mm and 140 mm width, respectively. During the first rotations, the axial core starts to form and the stripe widths shrink by a few percent. The tube length is 662 mm, the images show the full length of the tube on the horizontal axis. The initial distance of the stripes is (a) 40 mm, (b) 80 mm, (c) 120 mm, and (d) 160 mm. In all these experiments, the small stripe disappears.

of the regions of small beads. In Fig. 7(b), it is also evident that the dynamics of the central (dissolving) stripe changes considerably, after a new stripe of small particles has formed at the tube end. This is quantitatively discussed in the context of Fig. 12, below.

In order to study the interactions of individual bands via the core structure, two-stripe patterns have been prepared. Figures 8 and 9 show experiments using these initial conditions. Configurations with the same stripe widths but different stripe distances have been compared (Fig. 8), and the influence of different width ratios at a given stripe distance has been studied [see Figs. 9(a) and 9(d)]. Initially, an axial core of small-sized particles forms from the bands of small-grained material. Without exception, the prepared two-stripe pattern finally develops into a single-stripe configuration in our experiments. The width of the final stripe is somewhat smaller than that of the sum of the initial stripes. The difference is contained in an axial core that has formed in the course of the experiment.

Measurements of prepared stripes with different distances show that the time for the merging of stripes is directly related to the gap between the small-bead segments. For a quantitative analysis, we have performed a set of experiments at identical rotation speeds of 15 rpm and determined the relation between the initial stripe distance and the velocity of the stripe dissolution. This velocity is determined from

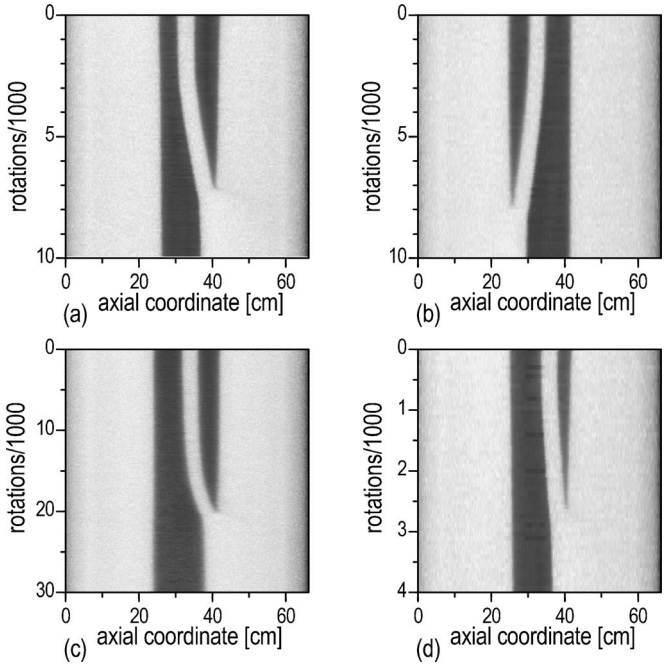

FIG. 9. Space-time plots of experiments in a 662 mm tube, initial stripe distance of 40 mm in all experiments, and different initial stripe widths: (a) 60 mm and 80 mm, mixture *L* (1:3), 15 rpm; (b) 60 mm and 80 mm, mixture *L* (1:3), 30 rpm; (c) 80 mm and 60 mm, mixture *S* (1:2), 20 rpm; (d) 93 mm and 47 mm, mixture *L* (1:3), 15 rpm.

the shift of the central band of large beads (central bright region in the plots of Fig. 8). This shift is proportional to the loss of small particles in the shrinking stripe and the gain of small particles in the growing stripe, and thus to the particle transport through the core channel. The dissolution process starts slowly after some "incubation period," and increases until it reaches some constant limit velocity. This is evidenced in all pictures of Fig. 8 by the parallel and relatively straight slopes of the borders of the central bright band in the space-time plot.

Figure 10 shows how the velocity of the small-particle transport through the core is determined from the position of one of the edges of the central band of large beads. The retardation after the preparation, an incubation period, sets in with the time needed to form a core channel, which is initially not present in the prepared stripe configurations. We note, however, that the amount of material that fills the core is very small, so that a quantitative observation of the related decrement of stripe widths proved, in general, impossible. Some loss connected with the core filling was indicated just for stripes with the largest distances studied, $d=160$ mm. A certain time after the core channel linking the bands has been established, one stripe begins to dissolve and material is transported into the other stripe. There was no clear relation between the geometry of the prepared pattern and the length of the incubation period, although a tendency towards longer incubation periods for larger separations d is evident.

The solid line in the diagram of Fig. 10(b) symbolizes the asymptotic velocity of the shrinkage process. The obtained asymptotic velocities of stripe dissolution as a function of the

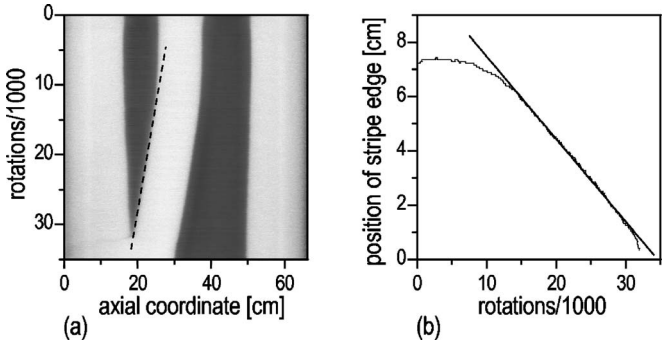

FIG. 10. Prepared stripe pair in a 662 mm tube, stripe distance 120 mm; the initial stripe widths are 105 mm and 140 mm, mixture *L* (1:3), 15 rpm. The image on the left shows the stripe dissolution; the image on the right presents the position of the inner edge of the left-hand stripe as a function of the number of rotations. The asymptotic dissolution velocity is taken from the tangent to the slope (straight line).

stripe distance d of the small bead stripes are displayed in Fig. 11. One can immediately see that the separation d has a crucial influence on the rate of the particle transport. As one may have guessed intuitively, the increasing length of the core channel slows down the transport rate of material through the channel under otherwise identical conditions. More interesting, however, is the result that the ratio of the stripe widths is obviously not relevant for the transport efficiency. Data for initial stripe ratios of 1:2 and 3:4 yield comparable transport rates. Intuitively, one might have assumed that relatively narrow stripes will lose their material much faster to a broader neighbor than stripes that have widths close to that of the competitor.

In order to test the hypothesis that the transport rate is inversely proportional to the channel length, we have plotted the inverse transport rate $1/v$ in all two-stripe experiments in

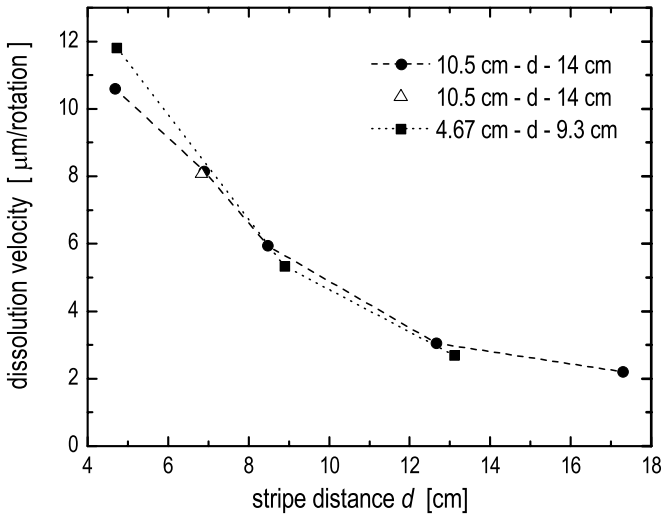

FIG. 11. Velocity v of the dissolution of the stripes as a function of the stripe distance d. Data are from stripe pairs with initial width ratios of approximately 3:4 (solid spheres) and 1:2 (solid squares); one datum point (open triangle) is from an experiment where the broader stripe dissolves; all other data originate from the dissolution of the narrower stripes.

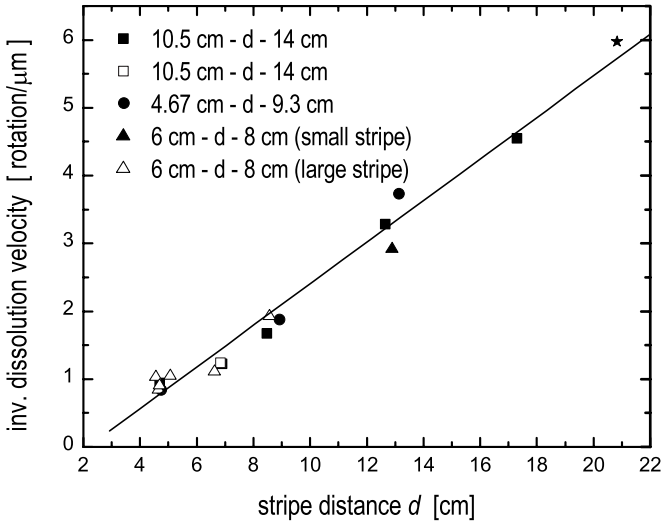

FIG. 12. Inverse transport rate $1/v$ in two-stripe systems as a function of the stripe distance d for different initial stripe widths. The solid line suggests a $v \propto 1/d$ dependence, which obviously holds independent of which stripe dissolves.

dependence upon the separation d in Fig. 12. The solid line is a linear fit of $1/v$ as a function of the distance d of the small bead bands. The choice of this simple fit function is empirical. A model that describes this dependence quantitatively should also take into account the logarithmic decay of the number of stripes $N(r)$ with the number of rotations in spontaneously formed segregation patterns (Fig. 4), and establish some relation between both results. The absolute widths of the bands of small particles may influence this dependence as well, although there is no evidence for such a dependence on absolute stripe widths in the data of Fig. 12. For comparison, the velocity of core formation measured in the single-stripe experiments (initial tangent to the single-stripes in Fig. 7) is 0.3 μm/rotation. The asterisk is taken from the dissolution rate of the stripe in Fig. 7(b) after the second stripe at the border has formed.

An unambiguous conclusion from the experiments with prepared stripes is that the dissolution of stripes is an irreversible process. This confirms our earlier hypothesis from the observation of spontaneously developed patterns. In most preparations, the larger stripe grows at the expense of the smaller competitor (cf. Fig. 8). The transport of material is rather slow in the beginning of the experiment, but in the course of the dissolution process, the transport becomes faster. In no case, was there a slowing down or even reversal of the drift, once initiated.

One may have the impression that with a few exceptions, the direction of material transport in the coarsening process is always from the narrower towards the broader bands. However, it is necessary to refer to some important exceptions observed in the experiment: In sequences of experiments performed under identical preparation conditions, we find almost exclusively the dissolution of the same stripe. When the ratio of stripe widths exceeded 2, we found no example of the dissolution of the broader stripe in a pair, thus for most parameter sets, the broader stripe "wins." In experiments with an initial 3:4 (105 to 140 mm) stripe pair, there was one of six experiments (see Fig. 11) where the narrower stripe succeeded. It turned out, however, that in some other experiments the broader stripe "lost" regularly; one of these situations is depicted in Fig. 9(a). The experiment was carefully repeated under identical conditions, and in order to exclude any influences of the direction of the filling process, we have also compared the mirror situations (narrow stripe filled in first and last, respectively). In all four experiments under the conditions of Fig. 9(a), the dissolution of the *broader* stripe was observed, and statistically it seems quite impossible that the losing stripe was selected by chance there. Only in a few exceptions, particularly when the initial stripe widths did not differ more than 30%, could we observe both scenarios (dissolution of the narrow stripe or broad stripe) in pairs prepared with the same parameters. When the stripes have initially almost the same sizes, the selection of the winning stripe seems to be random. Nevertheless, once a stripe in the pair was spontaneously selected to grow, the direction of material redistribution was never reversed. This makes clear that the initial ratio of stripe widths is not the exclusive factor that determines the direction of transport. So far, experiments with a variety of stripe width ratios, distances, and rotation speeds gave no clear general picture of the relation between the geometrical preparation parameters and the selection mechanism. Much more systematic experiments are necessary here. The observed irreversibility, however, suggests that the flow of material through the channel influences the structure of the core and/or the bands, such that in turn, the direction of transport becomes fixed. As a consequence, the initial selection of the winning stripe is final. Once the transport of material is observable in the optical images, the losing stripe is doomed, even if it is still broader than its opponent.

In order to answer the question of how the transport direction in the core channel is encoded in the segregation structure, one has to look for another (geometrical) factor that determines the redistribution of material, in addition to the ratio of stripe widths. This question can be answered best in the prepared two-stripe systems. It is clear that in the dynamics of the complex textures originating from homogeneous mixtures, Fig. 5, the situation is somewhat different. Some stripes start to grow initially and shrink later. But in this situation one has to take into account the competing interactions with left and right neighbors. The interactions between two single stripes are hardly separable. Since in these arrangements of arrays of bands, the dynamics involves a complex coupled growth and shrinkage of multiple bands, the irreversibility of the individual transport processes can be obstructed.

When an ensemble of equidistant and equally broad stripes is prepared, the selection of the winning stripes is much slower than for stripes that differ largely in size. This is an indication that the selection of the winning stripes occurs there in the consequence of small random fluctuations. Figure 13(a) shows the initial evolution of a seven-stripe array, with distances of 50 mm and widths of ≈50 mm. The pattern remains stationary over a period of more than 40 000 rotations, before the first stripe decomposes. This is almost one order of magnitude longer than the incubation period in the roughly comparable experiments of Fig. 9(c) with un-

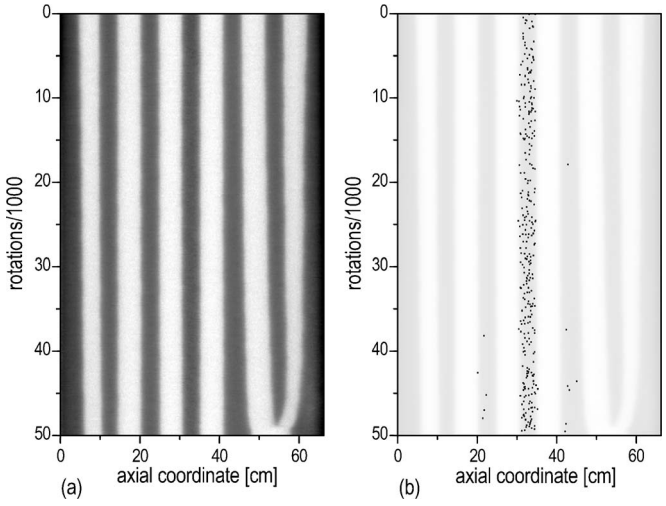

FIG. 13. (a) Experiment with a prepared array of seven equidistant identical stripes (mixture *S*, radius ratio 1:2). (b) Visualization of tracer particles by image processing (see the text). The tracers stay almost exclusively in the stripe where they have been deposited. Exchange with neighbor stripes is negligible unless a stripe dissolves.

equal stripe pairs. The experiment shown in Fig. 13 has been used to test the efficiency of the material redistribution through the core. We have doped one of the stripes of fine-grained material with beads of a different color. Approximately 100 beads have been placed on a selected stripe before the rotation experiment has been continued. The black tracer particles cannot be distinguished from the background of small-sized beads in the contrast-enhanced grayscale image of Fig. 13(a). Figure 13(b) shows the same experiment as Fig. 13(a) after digital-image processing: In each line, we mark by black dots the axial positions where at least one tracer particle has been detected in the image. Since the black markers may be submerged beneath the granulate surface, one detects only a small fraction of tracers in each image. Still, the statistics of visible tracer positions gives a qualitative picture of the tracer distribution. For comparison with the band positions, we have overlayed the tracer positions to a low-contrast copy of Fig. 13(a). One can follow the redistribution of markers between the neighboring bands of small beads during the pattern evolution. It turns out that in a stationary-stripe pattern, the markers remain almost completely in the original stripe. There is practically no diffusion of marked beads into neighboring stripes before the stripe dissolves. As long as the stripes remain stationary, practically all tracers stay in their original stripe. In contrast, a vanishing stripe distributes its tracers during the dissolution process completely among the neighboring, winning stripes. This result indicates that the essential process leading to the pattern dynamics is not a diffusive exchange of material between the small-bead bands through the core, but rather a unidirectional transport that leads to the dissolution of individual stripes in the pattern. The markers distribute approximately with the same velocity as the stripe dissolution process proceeds. Since the markers are not always visible at the surface of the granulate, the optical analysis can give, at the present stage, only a qualitative picture of the marker diffusion, but it is clear from Fig. 13(b) that only a few particles are lost by the original stripe during the observation period of some 50 000 rotations. In the moment the stripe dissolves (not shown here), it distributes all tracers among the neighboring stripes.

In view of the above-described observations, it seems appropriate to take a closer look at the evolution of individual stripes and the process of their dissolution. Two facts observed in the prepared systems of stripe pairs have to be combined: (1) the observation that the dissolution of a stripe, once initiated, is irreversible and (2) the fact that the initial selection of the winning stripe is not exclusively determined by the relative stripe widths. In some experiments, particularly when the ratio of stripe widths was smaller than two, the broader stripe became extinct. In that case, the stripe-width ratio is inverted during the dissolution process, so there must be other structural details of the segregation pattern that encode the particle-transport direction and mark the "doomed" band.

V. THREE-DIMENSIONAL STRUCTURE ANALYSIS

An established method to probe the detailed geometry of segregation patterns in a rotating drum is nuclear MRI. The distribution of water in the drum can be monitored in the MR images and the positions of the NMR-invisible granulate beads appear as "dark dots" in the images. The MRI measurement with the required resolution takes about 15 min, thus it was necessary to stop the rotation of the mixer during the MRI data acquisition and to detach it from the motor. The samples are prepared as in the optical experiment. Before the rotation starts, the initial particle distribution in the prepared stripes is monitored (Fig. 14, first image) by MRI. Then, the experiment is started. After a certain number of rotations, we stop again and place the drum into the MRI scanner. After the acquisition of the MRI data, the drum is connected to the motor again and the rotation is continued until the next interrupt for MRI measurements.

Figure 14 shows four sagittal slices, i.e., planes normal to the granulate surface, containing the axis of the tube, in a region of a prepared band of large beads (4 cm width), enclosed by two bands of small particles (8 and 6 cm widths, respectively). The MR images are slightly distorted towards the edges due to imperfect field homogeneity and the nonlinearity of the imaging gradient system outside the magnet's center. This artifact is not relevant for the evaluation of the images, and we have refrained from a digital correction. There are also some blurred dark spots in some images that represent artifacts, presumably small air bubbles trapped between the grains, which distort the local field.

The first image, Fig. 14(a), shows the prepared initial state. The bands are clearly separated and a core of small beads does not yet exist. The second image, Fig. 14(b), has been taken after 225 rotations at 15 rpm. One can see a symmetric core that extends between the two small-particle bands. The core also extends outwards from the outer edges of the small-bead bands. Figure 15 shows the same tube in the region at the right-hand side of the right stripe. In the third image, Fig. 14(c), taken after 4275 rotations, the pro-

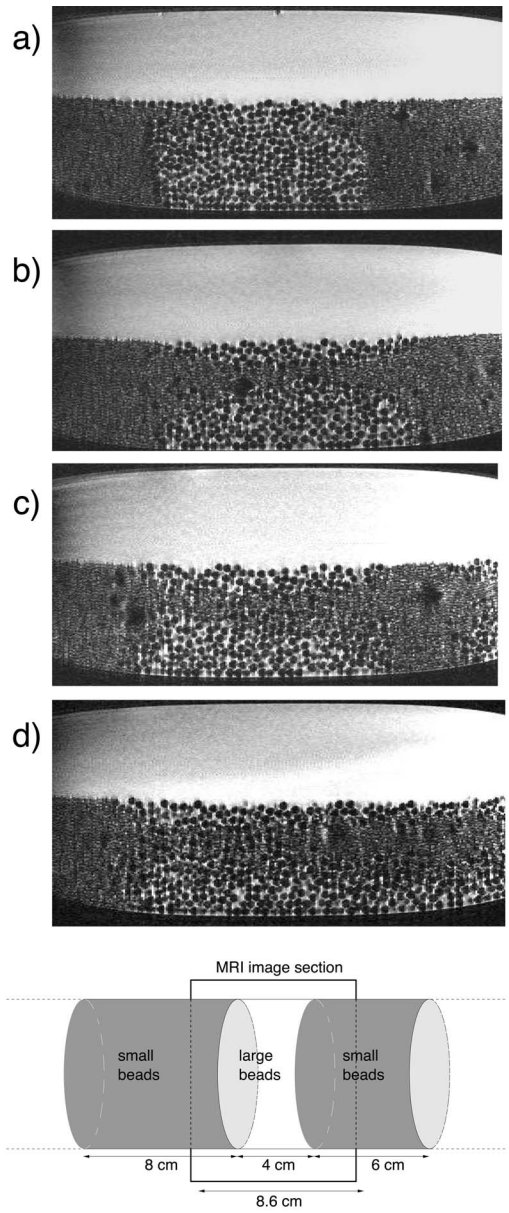

FIG. 14. MR images (sagittal sections) of a prepared two-stripe pattern (for details, see text), (a) before rotation, (b) after 225 rotations, (c) after 4275 rotations, and (d) after 4785 rotations. The right-hand stripe has disappeared optically after 4740 rotations. The bottom picture sketches the position of the MR image relative to the prepared pattern.

cess of dissolution of the stripe at the right-hand side is already in full effect. The remarkable feature of the core structure in this image is its obvious asymmetry. Finally, the fourth image, Fig. 14(d), shows the segregation pattern after 4785 rotations when in the optical images, the right-hand stripe has just disappeared. The small beads still form a massive cloud at the original position of the vanished stripe, but they are enclosed by large beads at the surface, thus they are no longer detected optically. This cloud persists for some time after the disappearance of the optical stripe; it distributes only gradually (Fig. 16).

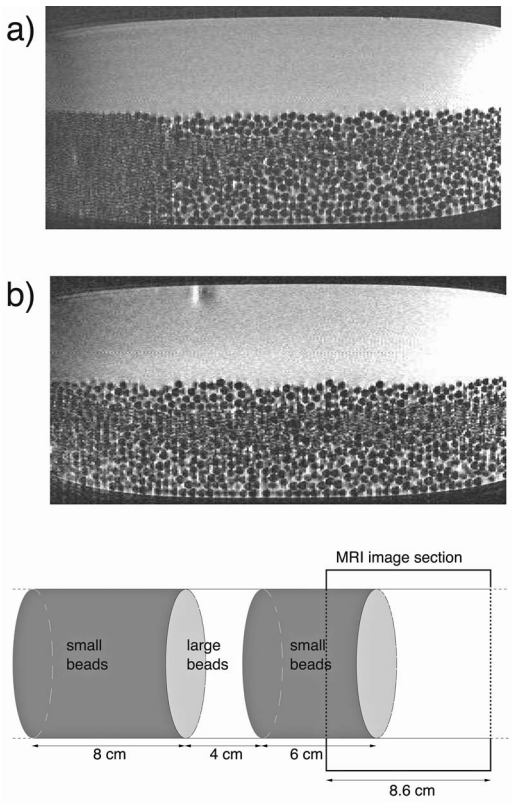

FIG. 15. MR images (sagittal cross section) of a prepared two-stripe pattern after 225 rotations (a) and after 4785 rotations (b), in the region to the right of the right-hand stripe.

It is also characteristic for all four images that not a single large bead has invaded the region of the left, persisting stripe of small beads. The same is evident in Fig. 15(a) and Fig. 16 [see also Fig. 17(a) described in the following paragraph]. In all these images, the small beads block the large beads from entering the bands.

The sagittal slices provide an illustrative overview of the 3D geometry of the bands, but they are not suitable for a quantitative evaluation, in particular, because they do not contain all information on the 3D core. Thus, we have evaluated the axial cross sections of the tube for a quantitative analysis. Such slices (perpendicular to the tube axis) can be taken in 0.5 mm steps. Figure 17 shows three typical axial slices of a prepared two-stripe pattern. These slices have

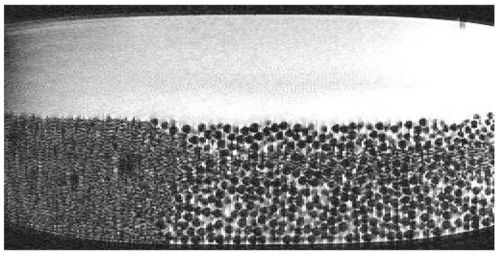

FIG. 16. MR image (sagittal cross section) of a prepared two-stripe pattern after 5500 rotations (at the same position as in Fig. 14). The right-hand stripe has disappeared.

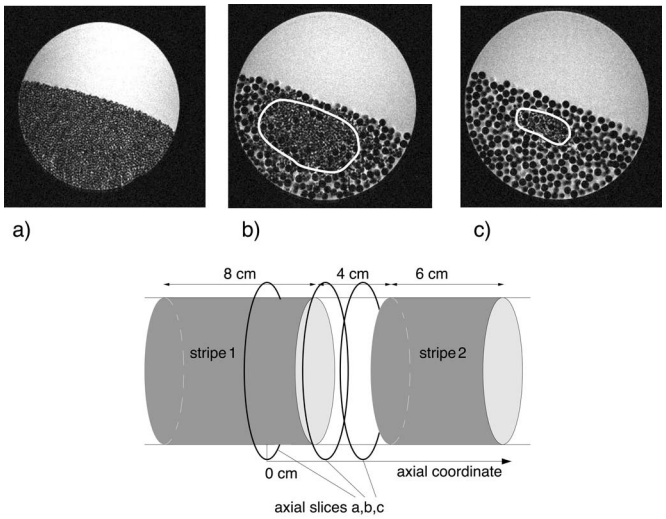

FIG. 17. MR images (axial sections) of a prepared stripe pattern consisting of two bands of small beads (8 cm and 6 cm), separated by a 4 cm band of large beads. The three axial slices are measured in the band of small beads (left), near the edge of the two bands (middle), and in the center of the band with large beads (right). The white lines in (b) and (c) mark the regions, which consist mainly of small-sized beads. The bottom image sketches the position of the three slices.

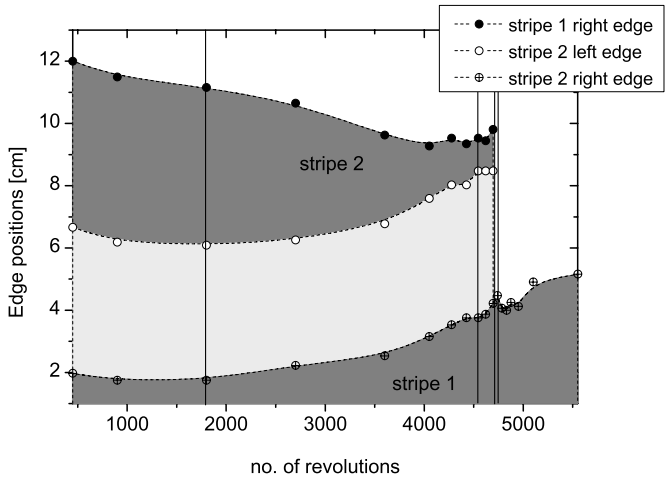

FIG. 19. Position of the bands in the prepared two-band pattern for the MRI measurements as seen from the surface, and their relation to the MRI data of Fig. 18. Open and solid circles symbolize the edges of the bands as determined optically. Shaded areas represent the regions of small particles (dark) and large particles (bright); they are meant merely to guide the eye. Vertical lines mark times where the cross sections of Fig. 18 have been taken.

been recorded in the middle of the band of small beads, near the edge of the band of small beads, and near the center of the band of large beads. In the first cross section, as expected, only the small beads are present, while in the other two slices one recognizes the core of small beads, surrounded by large beads. The geometry of this core can be defined rather precisely in these images. This core thins out gradually with increasing distance from the edge of the small-bead band.

Figure 18 shows the profiles of the core derived from the MRI data during the evolution of the segregation structure. A

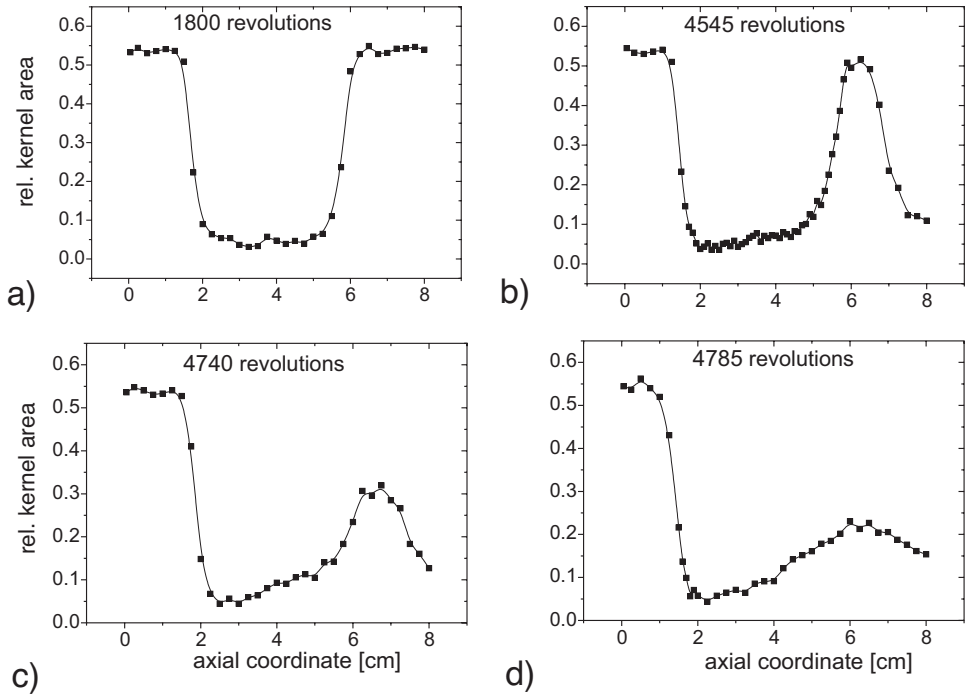

FIG. 18. Relative area covered by the small-sized beads in the axial MRI slices along the axis (related to the drum cross-section area). A coverage of 50% means that there are only small beads in the respective cross section; the rest is granulate-free (water). The development of the size and position of the two stripes in this experiment is shown in Fig. 19 where the instants at which MRI data have been sampled are marked by vertical lines.

set of axial slices has been analyzed digitally and the relative area covered by small beads (normalized by the cross section of the drum) has been determined. One of the initially prepared stripes disappears, and the geometry of the core changes during the redistribution process. Figure 19 shows the optical data of the stripe texture and vertical lines mark the time positions where the profiles in Fig. 18 have been evaluated from the MR images. The first profile, Fig. 18(a), taken after 1800 rotations, represents a situation where the initial stripe widths have not yet changed noticeably. The process of redistribution of the small beads between the two bands has not started yet. The axial core is already present; it links the two zones of small beads. The important geometrical aspect of the profile in Fig. 18(a) is that the core is symmetric on both sides. It covers at its narrowest part approximately 5% of the drum cross section. The stripe positions (Fig. 19) show that there is no net flow of small beads through the core channel. This feature appears to be related to the above-mentioned symmetry of the channel.

Figure 18(b) has been recorded after 4545 rotations. The process of the redistribution of small beads is fully developed (see Fig. 19). The particle flow through the axial core is directed from right to left in the cross sections of Fig. 18; the right band dissolves. In relation with this flow, the core profile has become asymmetric; the cross section of the axial core is approximately twice as large at the side of the dissolving stripe compared to the side of the gaining stripe. Figure 18(c) shows the profile when the right stripe has just vanished optically. The profile is clearly asymmetric. The last figure, Fig. 18(d), shows the same profile, only 45 rotations later. After the stripe has disappeared optically, the remaining submerged cluster of small beads dissolves much faster than during the preceding phase. The differences between the profiles Figs. 18(d) and 18(c) (45 rotations) are as dramatic as those during the preceding 200 rotations [profiles Figs. 18(c) and 18(b)].

In summary, the MRI data provide valuable information about the internal composition of the stripes. In particular, the images show that the small-bead regions in our mixture are completely free of large beads, which is important for the interpretation of the dynamics of the stripes, in general. It demonstrates that the small-bead bands block the redistribution of large beads so that the dynamics can be described as solely related to the redistribution of small beads. In addition, the MRI data allow us to establish a relation between the geometrical core structure and the direction of material transport.

VI. DISCUSSION AND SUMMARY

The macroscopic coarsening dynamics of segregation patterns of granular mixtures in a rotating drum represents a complex phenomenon, influenced by many parameters, such as the composition of the granulate, the ratios of the bead diameters, the filling factors of the tube, the presence or absence of an "immersion" liquid, rotation speeds, drum geometry, and many others. In the experiments performed here, we have focused on bimodal mixtures of glass beads in water, and most of the parameters have been kept fixed. We will discuss, in the following, which results are specific to the investigated system and which results can be generalized in our opinion.

The observation of segregation dynamics in the investigated slurry system at different rotation speeds reveals three qualitatively different regimes, and we have focused here on the regime of intermediate rotation frequencies where a nearly logarithmic coarsening dynamics is observed. We should note at this point that under identical conditions, the dry granular mixtures showed no axial segregation at all. This is in agreement with the findings in Ref. [22] that wet systems, in general, develop segregation patterns at lower rotation speeds than the dry counterparts. The systems investigated here are characterized by an almost-equal share of visible surface of small- and large-particle bands in the 50%:50% mixtures. The relative amount of visible small beads is slightly lower than 50%, but, in general, it varies only between 43% and 47%. This is a reasonable value that agrees with findings in comparable systems [22,23].

The logarithmic decay of the number of stripes in the segregation pattern with the number of rotations is found to be nearly independent of the rotation speed within a certain parameter range. A similar observation has been described in literature in a number of similar experiments, in dry and wet systems [22]. In our experiments, however, it has been shown that the logarithmic decay law holds only approximately, there is a clear tendency towards a faster decay rate with an increasing number of rotations or a decreasing number of remaining stripes. This detail becomes evident only in the measurements presented here because the experiments in this study have been performed over considerably longer periods than comparable studies in literature.

The mechanism of coarsening in the investigated system involves, exclusively, the redistribution of the small particles of the bidisperse mixture. This can be seen from the space-time plots where it is evident that the widths of large-bead regions trapped between two regions of small bands is constant in time. The MRI data confirm this assumption; the bands of small beads are completely free of large beads. One possible explanation that the bigger particles cannot cross the regions of the small-sized component is that the spherical monodisperse beads form some kind of dense packing where the big spheres represent defects. An argument that supports this interpretation is that the system of sand and big (2 mm) spheres shows a qualitatively different behavior. The large-sized spheres can easily pass the sand regions (Fig. 6) and redistribute. MRI measurements have not been performed in this system, but a close optical inspection of the sand-glass sphere mixture shows that all sand regions contain several percent of glass spheres, so there is no perfect segregation. This is also evident from the share of visible sand regions, which represent almost 60% of the total surface. Since sand and spheres were mixed in a 1:1 ratio, the segregated sand regions cannot be pure.

In the bidisperse mixture of glass spheres studied here, the segregation is nearly perfect, as the MR images show. There are no large-sized spheres in the compartments of small spheres, and small spheres are contained in the compartments of big spheres only in the core structure. The MR

images also show that the core structure has an irregular shape and no sharp boundaries. The small particles tunnel through the regions of large beads along the axial-core structure in the drum. This behavior facilitates the interpretation of the dynamic processes observed.

The restriction of the dynamics to the redistribution of the small-sized species cannot be generalized for all mixtures. For example, when the ratio of the glass-sphere diameters is closer to one, the segregation may be imperfect and the small-bead regions do not block the large beads from an axial redistribution. The dynamics is more complex in that case.

In a spontaneously formed complex stripe texture, the reconstruction of details of the coarsening processes is not easy. Even though some theoretical models for the coarsening dynamics have been proposed, largely phenomenologically, the relations between local stripe structures and stripe stabilities are not understood so far. In a given pattern, it is possible to predict the texture evolution only on a statistical level. The preparation of certain simple stripe arrangements, as for example, stripe pairs and regular stripe arrays, elucidates some important details of the coarsening process. The conclusions drawn from the experiments are as follows: The flow of material between the bands in the segregation pattern of the investigated bidisperse mixtures is restricted to the redistribution of the small-sized component through the core. The velocity of this particle transport is related to the distance between the bands of small beads. We find for the 3:1 mixture L that for given widths of the two commuting stripes, the rate of the dissolution process increases nearly linearly with their inverse distance $1/d$. On the other hand, the sizes of the two commuting stripes seem to be unimportant for the material flow and the velocity of the dissolution.

In an array of stripes of different widths, narrow stripes are, in general, less stable than broader neighbors. However, the dominance of broader stripes is decisive only if the difference in stripe widths is large enough (a factor of 2 or more). The transport of small-sized particles through the core structure, once initiated, is unidirectional, and it is coupled to a transformation of the core geometry. The core between a winning and a losing band of fine-grained material is funnel-shaped; the orientation of the funnel being related to the transport direction. The larger opening forms the source and the smaller opening forms the drain for net flow through the core. This geometrical transformation encodes the direction of transport, and once a flow direction is established, it is maintained until the losing stripe is extinguished. These conclusions on the unidirectional transport of small beads through the core structure are supported, qualitatively, by tracer observations.

It has been the aim of this work to direct attention to the study of the coarsening of granular segregation patterns from a general statistical point of view, to the analysis of the geometry of individual stripes. Detailed experimental information on the 3D structures in this particularly simple system is a prerequisite for the development of appropriate theoretical models that can describe the microscopic processes during the coarsening. The reproduction of the presented results, in particular, of the evolution of regular initial patterns, within numerical simulations, may provide a challenge for theoreticians, and may finally also lead to a better understanding of the coarsening dynamics of spontaneous-segregation patterns from homogeneous mixtures.

ACKNOWLEDGMENTS

The authors are particularly indebted to Susanne Kosanke for valuable contributions to the experiments, and to Thomas John for many useful discussions and technical support.

[1] G. H. Ristow, *Pattern Formation in Granular Material* (Springer, Berlin, 2000).
[2] L. P. Kadanoff, Rev. Mod. Phys. **71**, 435 (1999).
[3] H. M. Jaeger, S. R. Nagel, and R. P. Behringer, Rev. Mod. Phys. **68**, 1259 (1996).
[4] Y. Oyama, Sci. Pap. Inst. Phys. Chem. Res. (Jpn.) **6**, 600 (1939); **37**, 17 (1940).
[5] M. B. Donald and B. Roseman, Br. Chem. Eng. **7**, 749 (1962).
[6] S. das Gupta, D. V. Khakhar, and S. K. Batia, Chem. Eng. Sci. **46**, 1513 (1991).
[7] O. Zik, D. Levine, S. G. Lipson, S. Shtrikman, and J. Stavans, Phys. Rev. Lett. **73**, 644 (1994).
[8] Z. S. Khan, W. A. Tokaruk, and S. W. Morris, Europhys. Lett. **66**, 212 (2004).
[9] V. Frette and J. Stavans, Phys. Rev. E **56**, 6981 (1997).
[10] M. Nakagawa, S. A. Altobelli, C. Caprihan, E. Fukushima, and E.-K. Jeong, Exp. Fluids **16**, 54 (1993).
[11] M. Nakagawa, Chem. Eng. Sci. **49**, 2540 (1994).
[12] M. Nakagawa, S. A. Altobelli, C. Caprihan, and E. Fukushima, Chem. Eng. Sci. **52**, 4423 (1997).
[13] K. M. Hill and J. Kakalios, Phys. Rev. E **49**, R3610 (1994).
[14] K. M. Hill and J. Kakalios, Phys. Rev. E **52**, 4393 (1995).
[15] K. M. Hill, A. Caprihan, and J. Kakalios, Phys. Rev. Lett. **78**, 50 (1997).
[16] K. M. Hill, A. Caprihan, and J. Kakalios, Phys. Rev. E **56**, 4386 (1997).
[17] K. M. Hill, D. V. Khakbar, J. F. Gilchrist, J. J. McCarthy, and J. M. Ottino, Proc. Natl. Acad. Sci. U.S.A. **96**, 11701 (1999).
[18] K. M. Hill, N. Jain, and J. M. Ottino, Phys. Rev. E **64**, 011302 (2001).
[19] K. Choo, T. C. A. Molteno, and S. W. Morris, Phys. Rev. Lett. **79**, 2975 (1997).
[20] K. Choo, M. W. Baker, T. C. A. Molteno, and S. W. Morris, Phys. Rev. E **58**, 6115 (1998).
[21] N. Jain, D. V. Khakhar, R. Lueptow, and J. M. Ottino, Phys. Rev. Lett. **86**, 3771 (2001).
[22] S. J. Fiedor and J. M. Ottino, Phys. Rev. Lett. **91**, 244301 (2003).
[23] T. Arndt, T. Siegmann-Hegerfeld, S. J. Fiedor, J. M. Ottino, and R. M. Lueptow, Phys. Rev. E **71**, 011306 (2005).
[24] Z. S. Khan and S. W. Morris, Phys. Rev. Lett. **94**, 048002 (2005).

[25] A. Alexander, F. J. Muzzio, and T. Shinbrot, Granular Matter **5**, 171 (2004).
[26] L. Prigozhin and H. Kalman, Phys. Rev. E **57**, 2073 (1998).
[27] I. S. Aranson and L. S. Tsimring, Phys. Rev. Lett. **82**, 4643 (1999).
[28] I. S. Aranson, L. S. Tsimring, and V. M. Vinokur, Phys. Rev. E **60**, 1975 (1999).
[29] I. S. Aranson and L. S. Tsimring, Phys. Rev. E **65**, 061303 (2002).
[30] G. Baumann, I. M. Jánosi, and D. E. Wolf, Phys. Rev. E **51**, 1879 (1995).
[31] G. H. Ristow, Europhys. Lett. **34**, 263 (1996).
[32] S. N. Dorogovtsev, Europhys. Lett. **41**, 25 (1998).
[33] D. C. Rapaport, Phys. Rev. E **65**, 061306 (2002).
[34] T. Elperin and A. Vikhansky, Phys. Rev. E **60**, 1946 (1999).
[35] A. Awazu, Phys. Rev. Lett. **84**, 4585 (2000).
[36] S. Chakraborty, P. R. Nott, and J. R. Prakash, Eur. Phys. J. E **1**, 265 (2000).
[37] N. Taberlet, W. Losert, and P. Richard, Europhys. Lett. **68**, 522 (2004).
[38] R. Govindarjan, P. R. Nott, and S. Ramaswamy, Phys. Fluids **13**, 3517 (2001).
[39] D. Volfson, L. S. Tsimring, and I. S. Aranson, Phys. Rev. Lett. **90**, 254301 (2003); Phys. Rev. E **68**, 021301 (2003).
[40] In addition, there is also some interest in the dynamics of the fast speed (ballistic and centrifugal) regimes, see e.g., W. R. Matson, B. J. Ackerson, and P. Tong, Phys. Rev. E **67**, 050301(R) (2003); S. G. Lipson, J. Phys.: Condens. Matter **13**, 5001 (2001), and Refs. [41,42].
[41] A. P. J. Breu, C. A. Kruelle, and I. Rehberg, Europhys. Lett. **62**, 491 (2003).
[42] A. P. J. Breu, C. A. Kruelle, and I. Rehberg, Eur. Phys. J. E **13**, 189 (2004).
[43] J. Rajchenbach, E. Clement, and J. Duran, Europhys. Lett. **30**, 7 (1995); F. Cantelaube and D. Bideau, *ibid.* **30**, 133 (1995).
[44] We use the term, sagittal, here for vertical slices along the drum axis and the term, axial, refers to slices normal to that axis, according to the conventions of the MRI geometry.